Aligned Magnetic Field-Enhanced MHD Mixed Convection and Heat Transfer on a Moving Inclined Porous Surface

W. Sridhar[1*], D. Srinivasa Rao[2], G. Dharmaiah[3], V. Sujatha[1]
[1*]Department of Mathematics, Koneru Lakshmaiah Education Foundation, Vaddeswaram, Guntur, A.P., India
[2]Department of Mathematics, Aditya College of Engineering and Technology,Surampalem,E.G.Dist, A.P., India
[3]Department of Mathematics, Narsaraopet Engineering College, Narsaraopet, Guntur, A.P., India

Abstract: The primary objective of this study is to investigate the combined effects of magnetohydrodynamic (MHD) mixed convection flow and heat transfer on an inclined permeable sheet in motion, subjected to an aligned magnetic field. To attain this goal, precise solutions for the partial differential equations (PDEs) are derived using perturbation techniques.The research explores the impact of several factors, including thermal radiation, chemical reaction, Hall current, and the aligned magnetic field. Notably, it is observed that higher values of the Schmidt number (Sc) and the parameter γ lead to a reduction in fluid concentration. Conversely, elevated values of parameters ϕ, Prandtl number (Pr), and the mixed convection parameter (F) result in a decrease in temperature. The velocity of the fluid is found to increase with higher values of the Grashof numbers (Gr), Görtler numbers (Gc), thermal buoyancy parameter (α), mixed convection parameter (F), and the permeability parameter (K). On the contrary, the velocity decreases when parameters such as the Hartmann number (M), Sc, Pr, ξ, power-law index (m), and ϕ are increased. Further analysis reveals that the Sherwood number experiences a decline with increasing Sc and γ values. Conversely, the Nusselt number rises as the parameters F, ϕ, and Pr increase. Additionally, the study shows that an increase in the permeability parameter (K), Gr, and Gc results in a higher skin-friction coefficient, whereas an increase in parameters M, α, F, Sc, m, and ξ leads to a decrease in the skin-friction coefficient. To validate the findings, graphs are generated and compared with the calculated results. In summary, the study sheds light on the interplay between mixed convection, heat transfer, MHD effects, and aligned magnetic fields in a porous medium, providing valuable insights into the intricate fluid dynamics and thermal behavior.

Keywords: mixed convection, heat transfer, magnetohydrodynamics (MHD), aligned magnetic field, porous media

1. INTRODUCTION

The convection of heat and mass across inclined porous surfaces finds numerous applications across various scientific disciplines and technological domains, including chemical industries, nuclear reactor cooling, MHD power generation, geothermal energy extraction, and petroleum engineering. Contemporary research has placed a significant focus on investigating convective heat and mass transfer phenomena involving different physical properties, especially concerning horizontal and vertical flat plates. This study delves into the complex interplay of Hall current and aligned magnetic fluid flow through porous media. The research emphasizes the current relevance of thermal radiation's impact on unsteady forced convection when subjected to an aligned magnetic field. Magnetic and aligned electric fields emerge as crucial factors in fluid dynamics, enabling the dissociation of plasma elements by disrupting the frozen field condition. This phenomenon leads to the breakdown of equi-potential mapping, efficient particle acceleration, and swift release of magnetic energy. Several mechanisms, including wave turbulence, solitary structures, magnetic

mirrors, electric double layers, and dynamic trapping, contribute to the existence of aligned electric fields. Within the realm of collision-less space plasma, the presence of magnetic-field aligned electric fields holds immense significance. For brevity, the term "parallel" is employed interchangeably with "magnetic-field aligned." The persistence of a non-vanishing magnetic-field aligned electric field necessitates a continual balance of momentum imparted to charged particles. This equilibrium can manifest in various types of magnetic-field aligned electric fields, each characterized by specific features such as Forces originating from AC electric fields, Forces influenced by the DC magnetic field and Inertial forces.

Recent research has explored these concepts extensively. Chamkha et al. [1] conducted numerical examinations of chemical reactions and thermal radiation effects, while Rees and Pop [2] simulated variable permeability effects. Ingham et al. [3] analyzed viscous dissipation within a porous medium between parallel plates, and Umavathi et al. [4] studied unsteady oscillatory flow effects within a horizontal composite porous medium channel. Chamkha et al. [5] explored the impact of radiation on flows of non-Newtonian fluids with aiding and opposing eternal flows.
Despite these efforts, boundary layer flows adjacent to inclined plates have received less attention. Notably, Hossain [6] examined the effect of Ohmic heating on MHD free convection heat transfer in a Newtonian fluid. Additionally, studies by Hossain and Gorla [7], Beg et al. [8], Chen [9], Reddy et al. [10], Sibanda and Makinde [11], Wang et al. [12], Yia [13], Choudhury and Das [14], Raju et al. [15], and others contributed valuable insights to the field. The central aim of this article is to investigate the combined effects of mixed convection, thermal radiation, chemical reaction, Hall current, and aligned magnetic field on MHD flow of viscous, incompressible, and electrically-conducting fluid over a moving inclined porous plate. The intricate coupled partial differential equations are tackled using perturbation techniques, leading to analytical solutions.

2. MATHEMATICAL FORMULATION

Consider a free convective laminar boundary layer flow of a viscous incompressible electrically conducting, chemically reactive, radiative and heat absorbing fluid past a semi-infinite moving permeable plate inclined at an angle α a in vertical direction embedded in a uniform porous medium, which is subject to thermal and concentration buoyancy effects along with Joule's dissipation. The temperature of the wall is maintained T_w and concentration $C_w$which is higher than the ambient temperature T_∞ and concentration C_∞ respectively. Also it is assumed that there exists a homogeneous chemical reaction of first order with rate constant between the diffusing species and the fluid. With these physical considerations, the equations governing the fluid in Cartesian frame of reference are given below.

$$\frac{\partial v}{\partial y} = 0 \quad \Rightarrow \quad v^* = -V_0 \tag{1}$$

Momentum Equation

$$\rho v^* \frac{\partial u^*}{\partial y^*} = \mu \frac{\partial^2 u^*}{\partial y^{*2}} - \frac{\mu}{k^*} u^* - \frac{\sin^2 \xi}{1+m^2} \sigma B_0^2 u^* + \rho g \cos\alpha \, \beta_T (T^* - T_\infty) + \rho g \cos\alpha \, \beta_C (C^* - C_\infty) \tag{2}$$

Energy Equation

$$\rho C_p v^* \frac{\partial T^*}{\partial y^*} = \alpha_1 \frac{\partial^2 T^*}{\partial y^{*2}} + \mu \left(\frac{\partial u^*}{\partial y^*} \right)^2 - \frac{\partial q_r^*}{\partial y^*} + \frac{\sin^2 \xi}{1+m^2} \sigma B_0^2 u^{*2} - Q_0 (T^* - T_\infty) \tag{3}$$

Concentration Equation

$$v^* \frac{\partial C^*}{\partial y^*} = D \frac{\partial^2 C^*}{\partial y^{*2}} - R(C^* - C_\infty) \tag{4}$$

The radiative heat flux

$$\frac{\partial q_r^*}{\partial y^*} = 4(T^* - T_\infty) I' \tag{5}$$

Where $I' = \int_0^\infty K_{\lambda w} \frac{\partial e_{b\lambda}}{\partial T^*} d\lambda$, $K_{\lambda w}$ is the absorption coefficient at the wall and $e_{b\lambda}$ is Plank's function.

Under these assumptions the appropriate boundary conditions for velocity, temperature and concentration fields are defined as

$$u^* = 0, \quad T^* = T_\infty, \quad C^* = C_\infty \qquad at \quad y = 0 \tag{6}$$

$$u^* \to 0, \quad T^* \to T_\infty, \quad C^* \to C_\infty \qquad as \quad y \to \infty \tag{7}$$

Introducing the following non-dimensional quantities

$$u = \frac{u^*}{v_0}, \upsilon = \frac{\mu}{\rho}, R_1 = \frac{\upsilon(C_w - C_\infty)R_A}{v_0^2 \rho C_p (T_w - T_\infty)}, y = \frac{v_0 y^*}{\upsilon}, u_p = \frac{u_p^*}{v_0}, M^2 = \frac{B_0^2 \upsilon^2 \sigma}{v_0^2 \mu}, K = \frac{K^* v_0^2}{\upsilon^2},$$

$$\theta = \frac{T^* - T_\infty}{T_w - T_\infty}, C = \frac{C^* - C_\infty}{C_w - C_\infty}, Sc = \frac{\upsilon}{d}, \gamma = \frac{R\upsilon}{v_0^2}, \Pr = \frac{\mu Cp}{\alpha_1}, H = \frac{Q_0}{\rho C_p v_0^3}, F = \frac{4\upsilon I'}{\rho C_p v_0^2},$$

$$Ec = \frac{v_0^2}{C_p (T_w - T_\infty)}, Gr = \frac{\rho g \beta_T \upsilon^2 (T_w - T_\infty)}{v_0^3 \mu}, Gc = \frac{\rho g \beta_C \upsilon^2 (C_w - C_\infty)}{v_0^3 \mu} \tag{8}$$

Where the parameters are Grashof number Gr, modified Grashof number Gm, angle of inclination α, radiation parameter F, Schmidt number Sc, chemical reaction parameter γ , Hartmann number M, temperature dependent heat source parameter H, porosity parameter K, Prandtl number Pr, Schmidt number Sc, Hall current parameter m and the aligned angle ξ .

The basic field equations (2) – (4), can be expressed in non-dimensional form as:

$$\frac{\partial^2 u}{\partial y^2} + \frac{\partial u}{\partial y} - D_3 u = -D_1 \theta - D_2 C \tag{9}$$

$$\frac{\partial^2 \theta}{\partial y^2} + \Pr \frac{\partial \theta}{\partial y} + \Pr Ec \left(\frac{\partial u}{\partial y} \right)^2 + \Pr EcM_1 u^2 - \Pr(F + \phi) = 0 \tag{10}$$

$$\frac{\partial^2 C}{\partial y^2} + Sc \frac{\partial C}{\partial y} - Sc\, \gamma\, C = 0 \tag{11}$$

Where $D_1 = Gr \cos\alpha$; $D_2 = Gm \cos\alpha$; $\mathrm{M}_1 = \frac{M^2 \sin^2 \xi}{(1+m^2)}$; $D_3 = \frac{1}{K} + M_1$;

The corresponding boundary conditions in non-dimensional form are:

$$u = 0, \theta = 1, C = 1 \qquad at \quad y = 0 \tag{12}$$

$$u \to 0, \quad \theta \to 0, \quad C \to 0 \qquad as \quad y \to \infty \tag{13}$$

3. RESULTS AND DISCUSSIONS

The present study considers the effects of radiation absorption R_1 and chemical reaction γ , on transient free convection flow of heat and mass transfer in MHD free convective joule heating and radiative flow in a moving inclined porous surface with temperature dependent heat source. Solutions for velocity, temperature and concentration field are obtained by using perturbation technique with γ = 0.1,Ec = 0.01, Sc = 0.60, Pr = 0.7, M = 2.0, K = 0.5, Gc = 2.0, Gr = 4.0, $\alpha = \pi/6$, F =1.0, ϕ = 0.1, $\xi = \pi/4$and therefore, all the graphs corresponds to these unless specifically indicated on the appropriate graph. The effects of various parameters like Grashof number Gr, modified Grashof number Gc, angle of inclination α, radiation parameter F, Schmidt number Sc, chemical reaction parameter γ, Hartmann number M, heat source parameter ϕ, porosity parameter K, Prandtl number Pr, Schmidt number Sc, Hall current parameter m and the aligned angle ξ on velocity, temperature and concentration have been studied analytically and effects are executed with the help of figures. Also, the behaviors of the skin-friction, rate of heat transfer and the rate of mass transfer with respect to various parameters have been studied and the results were presented in Tables. The behavior of fluid velocity by the influence of M, K, α, Gr, Gc and F in Figs. 1- 6.

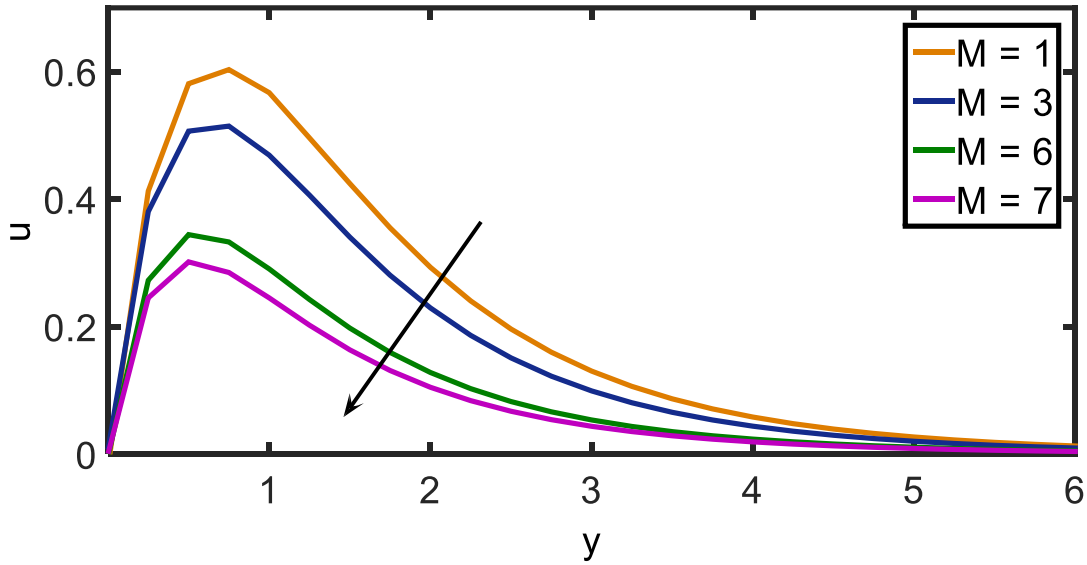

Figure 1: Velocity profiles for different values of Hartmann number M.

Figure 1 displays the effect of Hartmann number (M). It is noticed that as the values of M increase, the velocity profiles gradually decrease. The material science behind this may be elucidated in a way that the transverse attractive field toward the way average to an electrically-enthralling in fluid flow tends to influence a pulling to compel as the Lorenz force, which denies the smooth development of the liquid stream accomplishing a stream obstruction affect. With this reason, retardation in the velocity of the fluid and an increment in its boundary layer thick-ness. Figure 2 demonstrate that velocity profile for different values of porosity parameter (K). As K increases velocity also increases. The velocity profiles different values of Magnetic field direction angle α are depicted in Figure 3. It can be observed from the figure that the velocity decreases with an increasing value of α. Also, it is clear that the retardation force increases with increasing the

angle α. Figure 4 depicts that the effects of Grashof number (Gr) on velocity profile. From this figure it is noticed that the velocity increases as Grashof number increases. Figure 5 speaks to typical velocity profiles in the boundary layer for various values of the modified Grashof number (Gc). As expected, the fluid velocity increases and the peak value more distinctive due to increase in the concentration buoyancy effects represented by modified Grashof number. This is evident in the increase in the value of velocity as the modified Grashof number increases. Figure 6 shows the velocity profiles for different values of the radiation parameter (F), clearly as radiation parameter increases the peak values of the velocity tends to decreases. For different values of the Schmidt number (Sc) the velocity profiles are plotted in Figure 7. It is obvious that an increase in the Schmidt number results in decrease in the velocity within the boundary layer. Figure 8 represents the velocity profiles for different values of the Prandtl number. It is observed that the velocity decrease as an increasing the Prandtl number. The influence of the aligned angle ξ on the velocity profile is appeared in Figure 9. It is observed that an increase in the aligned angle ξ causes to decrease the fluid velocity. A velocity profile for different values of Hall current parameter (m) is shown in Figure 10.Asthe Hall current parameter (m) increases velocity distribution decreases. A velocity profile for different values of heat source parameter ϕ is appeared in Figure 11. As ϕ increases velocity distribution decreases. Figure 12 displays the effect of radiation parameter (F). It is seen that F increases temperature decreases; it is due to the fact that the conduction effect of the fluids decreases in the presence of radiation. Consequently, higher estimations of radiation parameter infer higher surface heat flux thus diminish the temperature inside the boundary layer vicinity. Figure 13 demonstrates the temperature profiles for various estimations of the Prandtl number. Prandtl number describes the relative ampleness of the energy transport by scattering in the hydrodynamic boundary layer to the centrality transported by thermal dispersion in the thermal boundary layer. As showed by the significance of Prandtl number higher Pr fluids brought down thermal conductivities which reduce the conduction heat transfer and increments temperature assortments at the surface. The Pr portrays the extent of energy and thermal diffusivity. The figure shows that an extension in Pr accomplishes diminishing temperature dispersion, since; thermal boundary layer thickness decreases with increasing values of Pr. Figure 14 employed to investigate the fluid flow effect of ϕ on temperature. From this figure, it is observed that the temperature decrease as an increasing the heat source parameter ϕ. Figure 15 shows the behavior concentration for different values of chemical reaction parameter γ. It is observed that an increase in leads to a decrease in the values of concentration. Figure 16 displays the effect of the Schmidt number Sc on the concentration profiles. As the Schmidt number increases the concentration decreases.

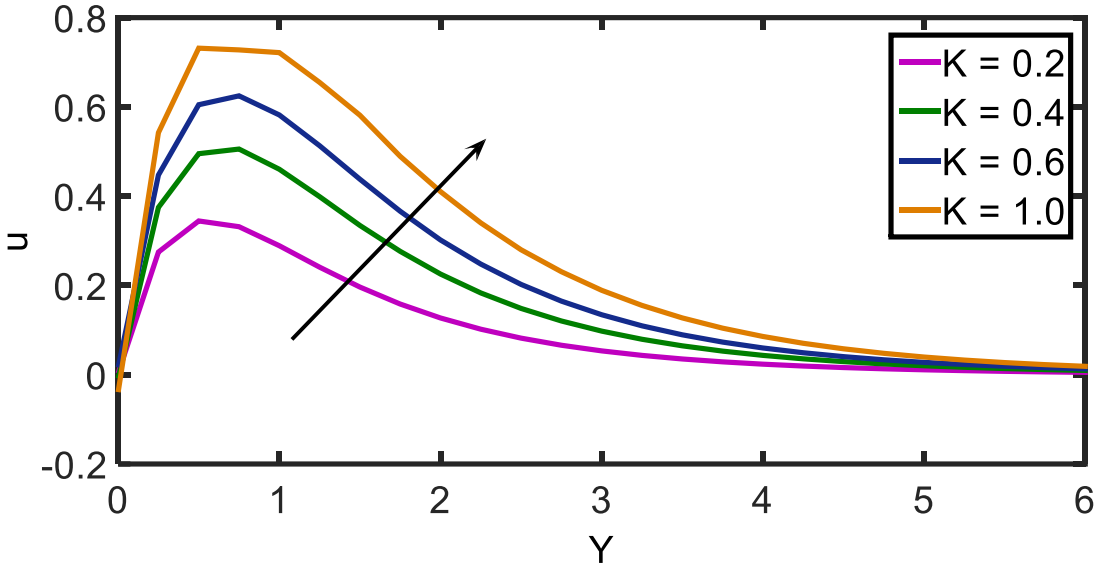

Figure 2: Velocity profiles for different values of the porosity parameter K.

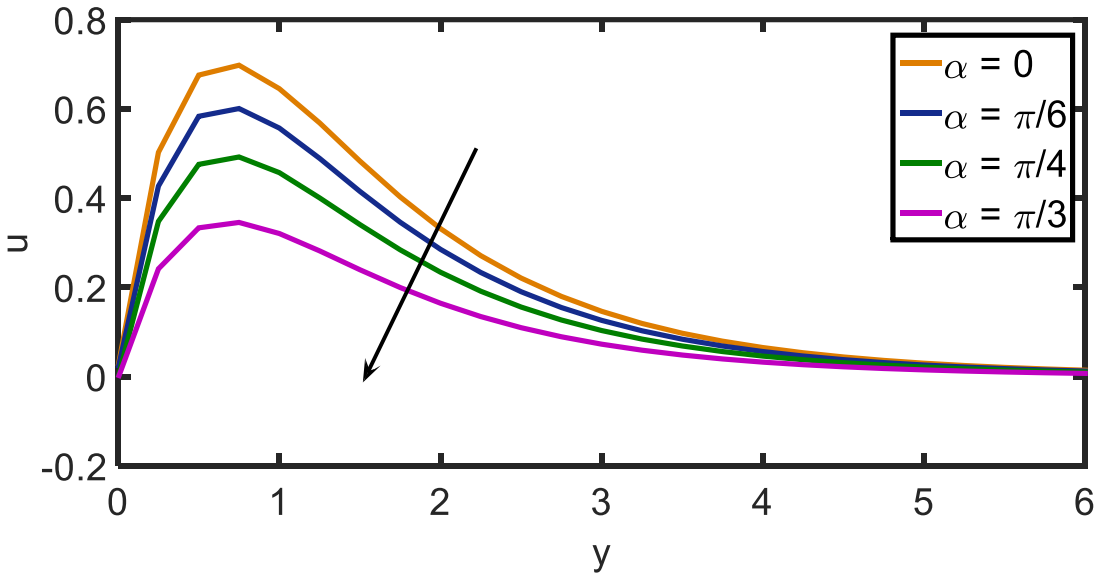

Figure 3: Velocity profiles for different values of the angle of inclination α.

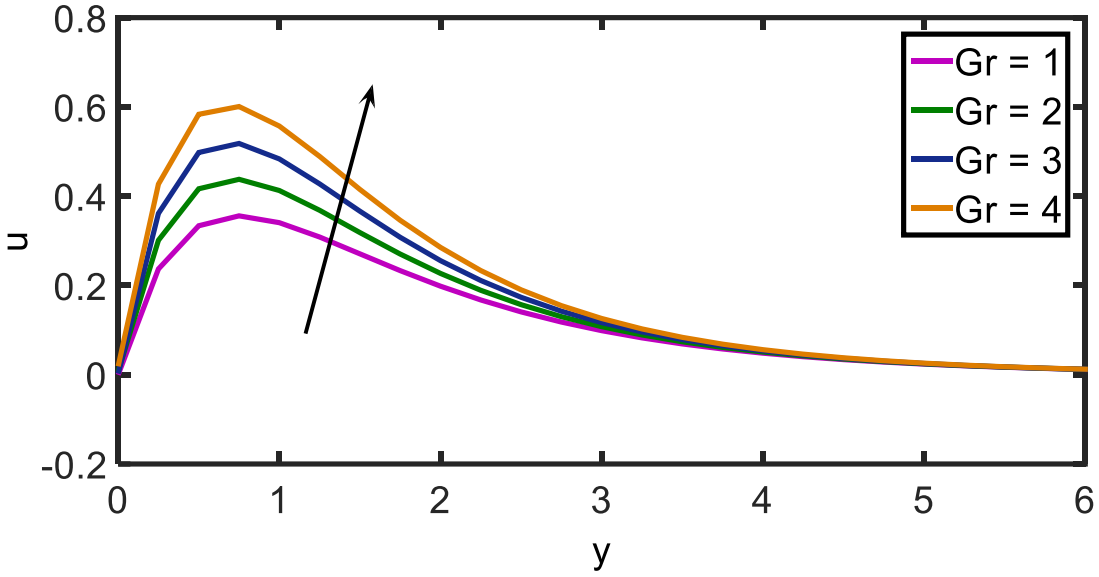

Figure 4: Velocity profiles for different values of the Grashof number Gr.

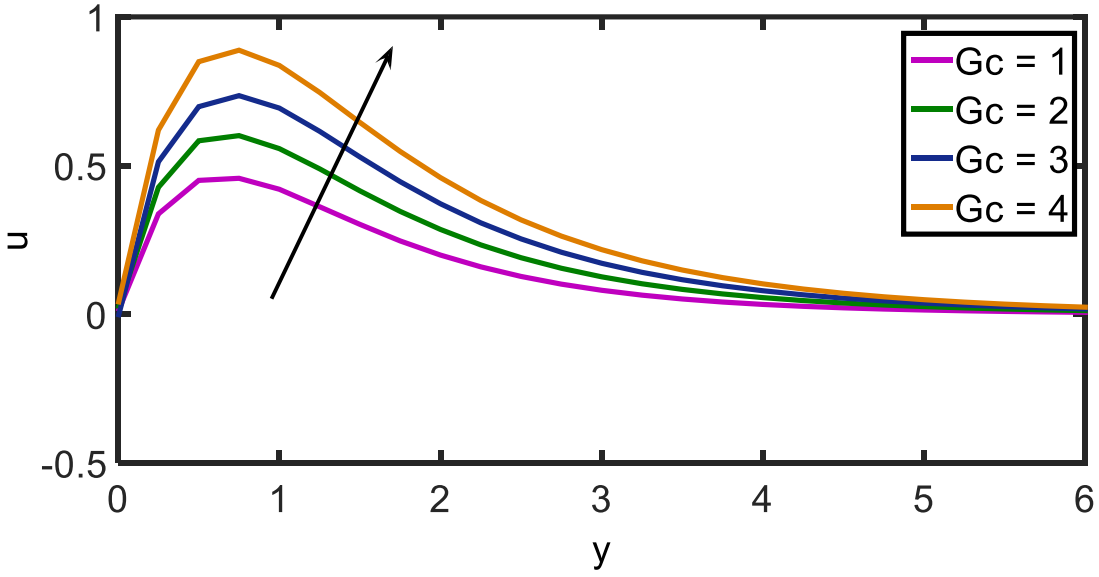

Figure 5: Velocity profiles for different values of the modified Grashof number Gc

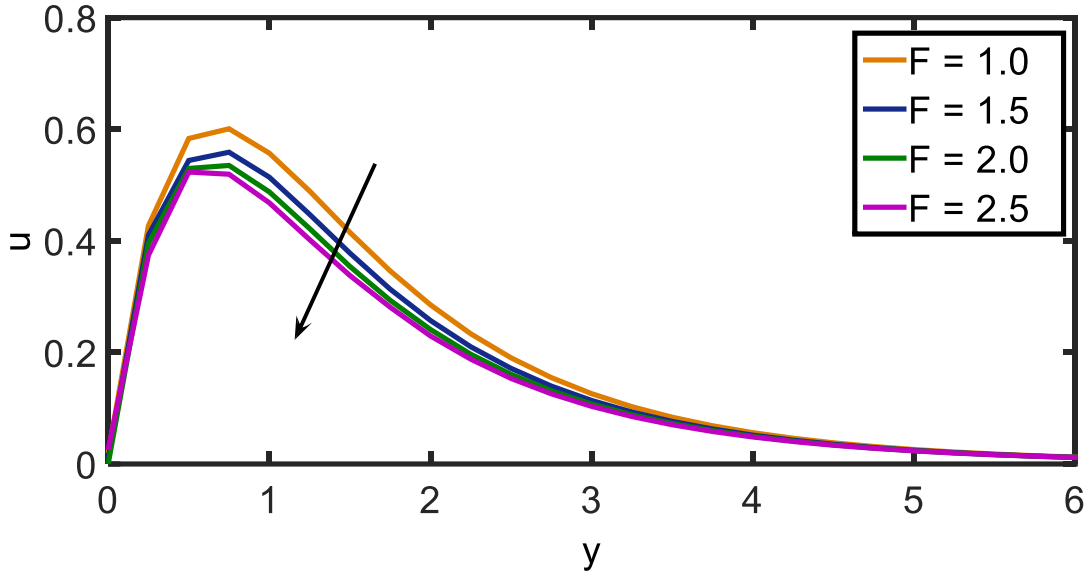

Figure 6: Velocity profiles for different values of the radiation parameter F.

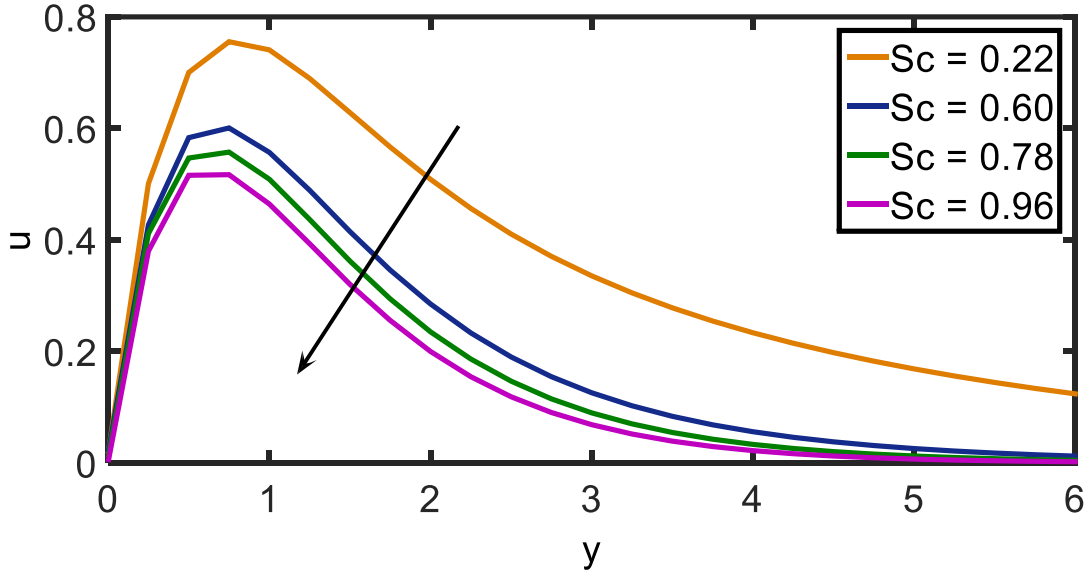

Figure 7: Velocity profiles for different values of the Schmidt number Sc

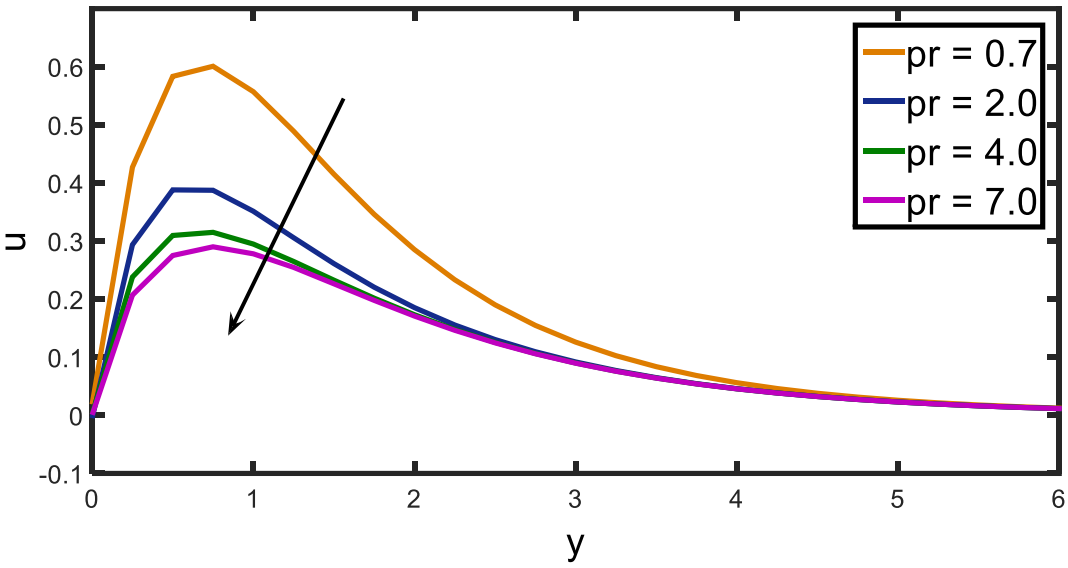

Figure 8: Velocity profiles for different values of the Prandtl number Pr.

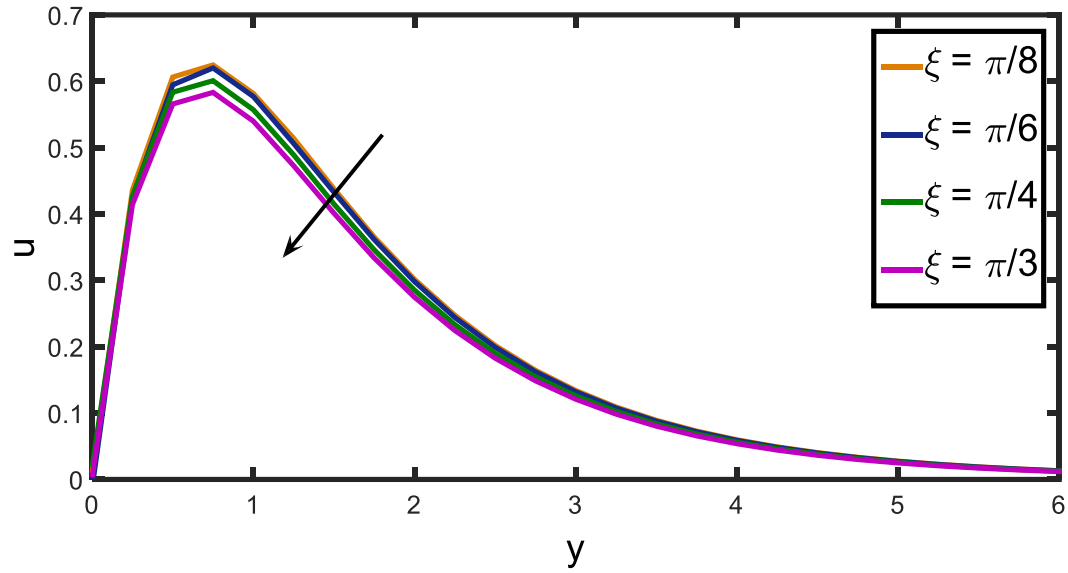

Figure 9: Velocity profiles for different values of the aligned angle ξ.

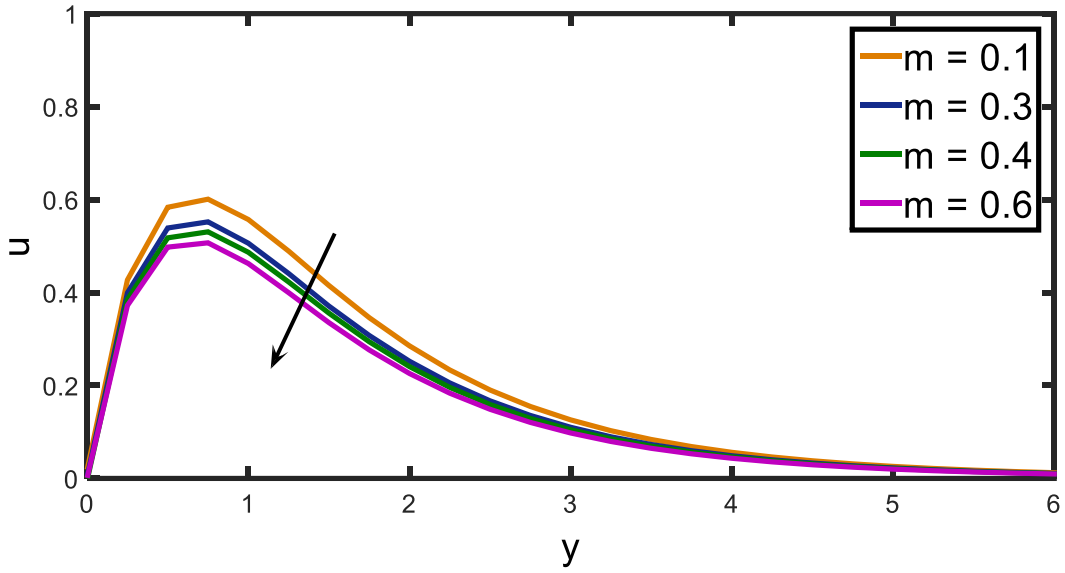

Figure 10: Velocity profiles for different values of the Hall current parameter m.

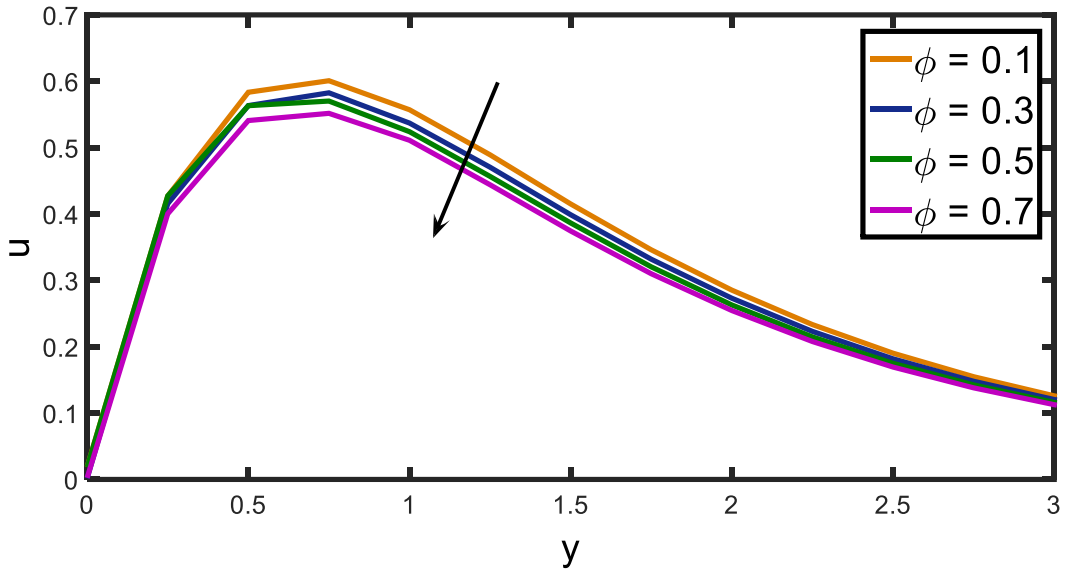

Figure 11: Velocity profiles for different values of the heat source parameter ϕ.

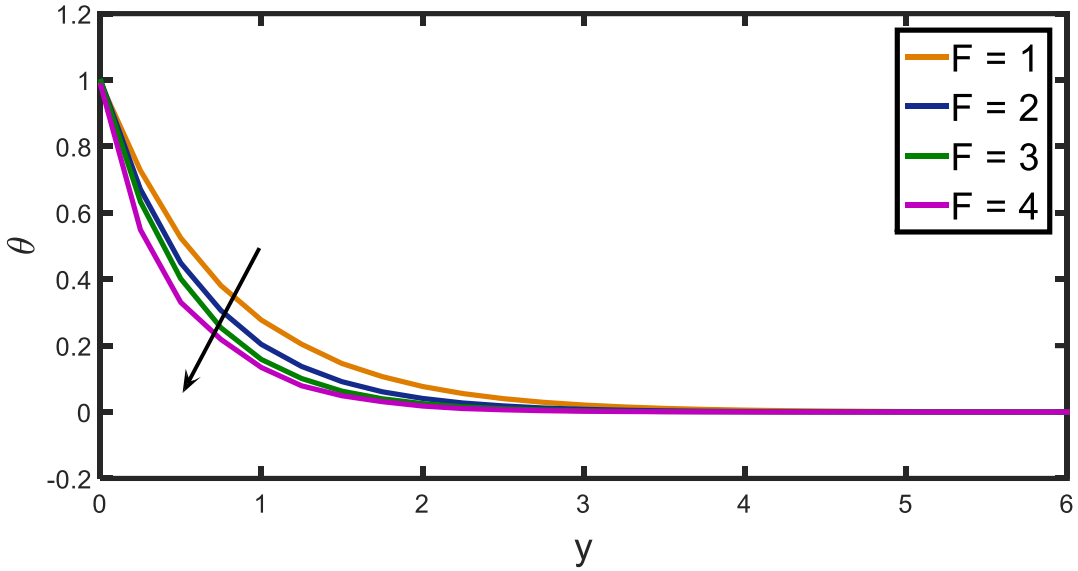

Figure 12: Temperature profiles for different values of the radiation parameter F.

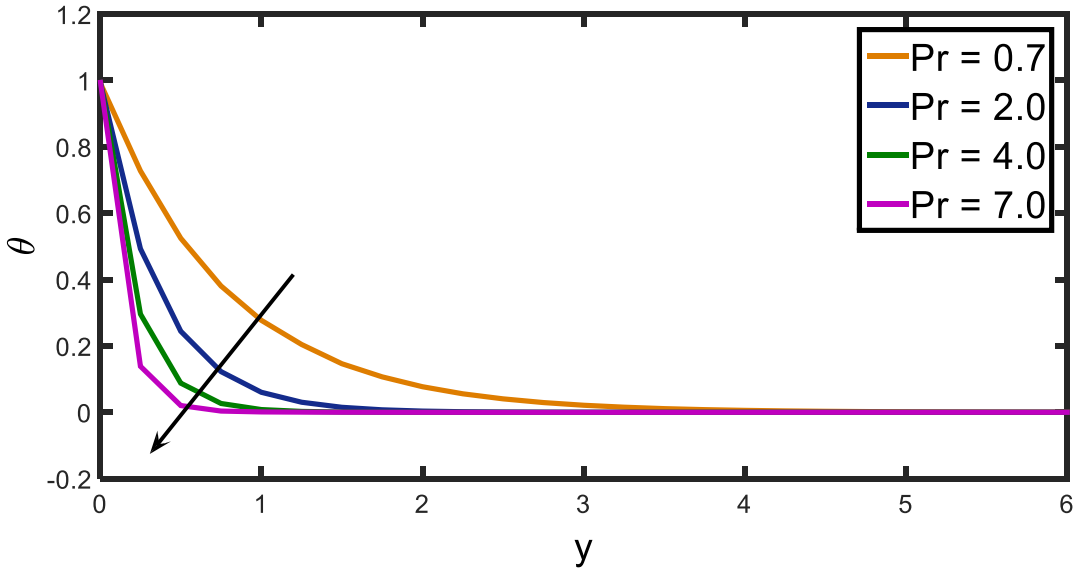

Figure 13: Temperature profiles for different values of the Prandtl number Pr.

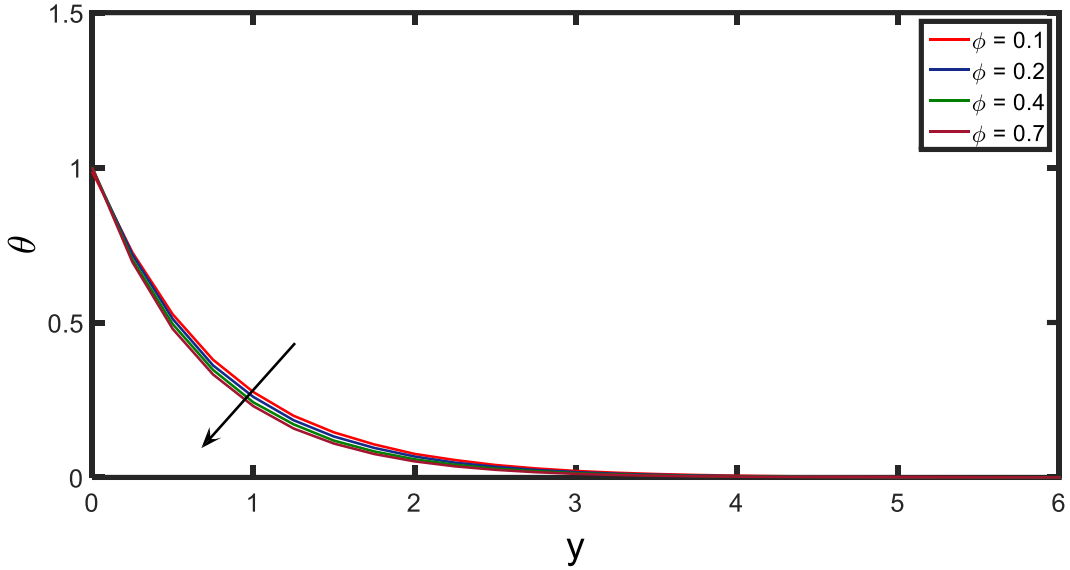

Figure 14: Temperature profiles for various values of the heat source parameter ϕ.

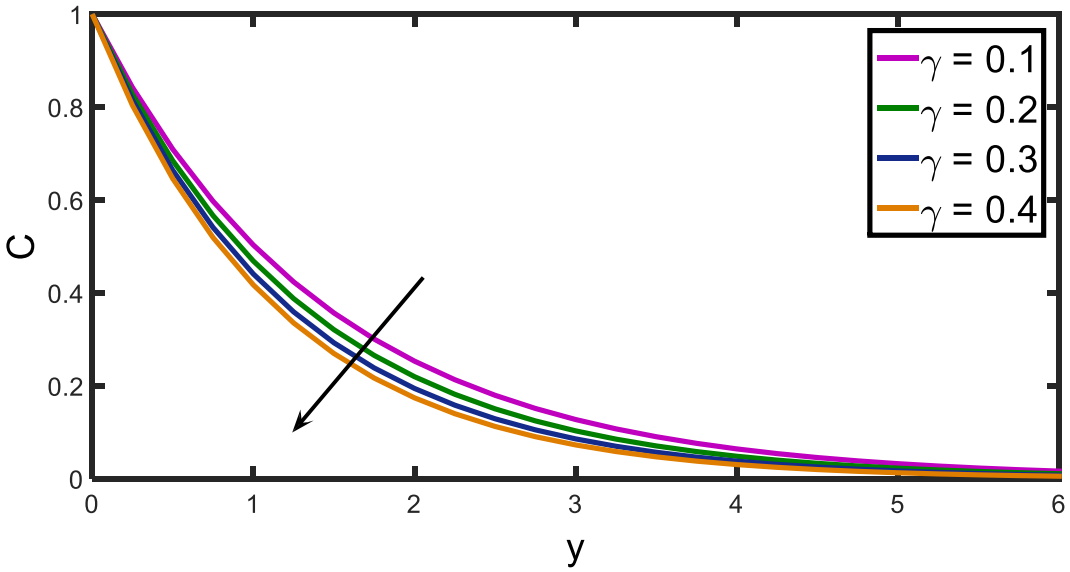

Figure 15: Concentration profiles for different values of the chemical reaction parameter γ.

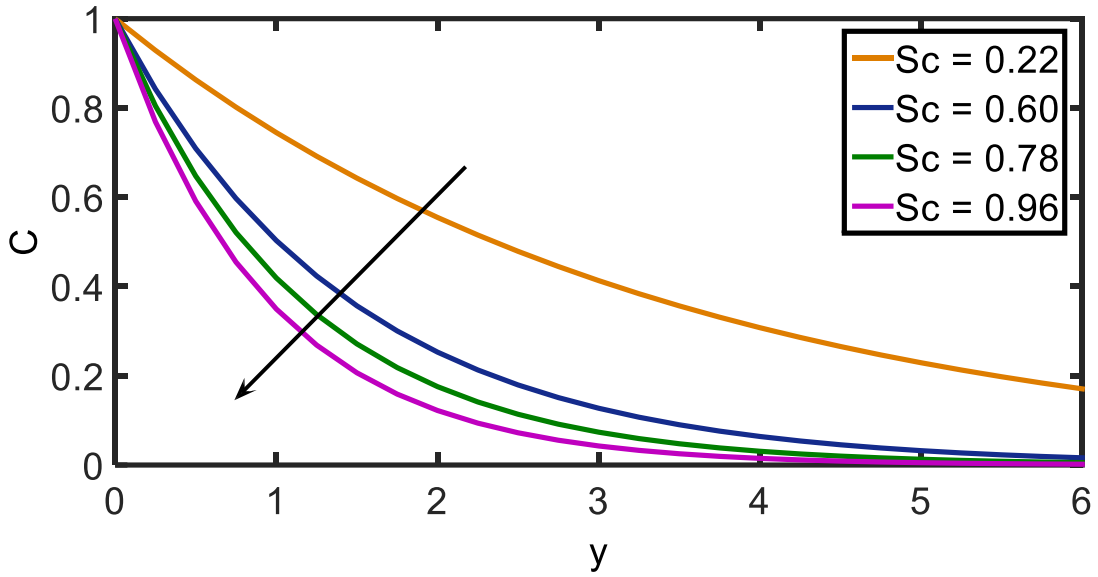

Figure 16: Concentration profiles for different values of the Schmidt number Sc.

From Table 1, we conclude that increasing of K, Gr, Gc causes the skin-friction coefficient to increase. Also, upon increasing of M, α, F, Sc, m and ξ, the skin-friction decreases. From Table 2, it is observed that upon increasing of Pr, F and ϕ the Nusselt number increases. From Table 3, we conclude that increasing of Sc, γ causes the Sherwood number to decrease.

Table 1: The effects of various parameters on the skin-friction coefficient

M	**K**	**α**	**Gr**	**Gc**	**F**	**Sc**	**ξ**	**m**	**τ**
2.0	0.5	π/6	4.0	2.0	1.0	0.60	π/4	0.1	2.4355
4.0	0.5	π/6	4.0	2.0	1.0	0.60	π/4	0.1	2.2518
5.0	0.5	π/6	4.0	2.0	1.0	0.60	π/4	0.1	2.1895
2.0	**0.2**	π/6	4.0	2.0	1.0	0.60	π/4	0.2	1.7640
2.0	**0.4**	π/6	4.0	2.0	1.0	0.60	π/4	0.2	2.2138
2.0	**0.6**	π/6	4.0	2.0	1.0	0.60	π/4	0.2	2.5238
2.0	**0.9**	π/6	4.0	2.0	1.0	0.60	π/4	0.1	2.8048
2.0	0.5	**0**	4.0	2.0	1.0	0.60	π/4	0.1	2.8018
2.0	0.5	**π/4**	4.0	2.0	1.0	0.60	π/4	0.1	2.0406
2.0	0.5	**π/3**	4.0	2.0	1.0	0.60	π/4	0.1	1.4298
2.0	0.5	π/6	**1.0**	2.0	1.0	0.60	π/4	0.1	1.3586
2.0	0.5	π/6	**2.0**	2.0	1.0	0.60	π/4	0.1	1.7078
2.0	0.5	π/6	**3.0**	2.0	1.0	0.60	π/4	0.1	2.0941
2.0	0.5	π/6	4.0	**3.0**	1.0	0.60	π/4	0.1	3.0063
2.0	0.5	π/6	4.0	**4.0**	1.0	0.60	π/4	0.1	3.3969
2.0	0.5	π/6	4.0	**5.0**	1.0	0.60	π/4	0.1	3.9472
2.0	0.5	π/6	4.0	2.0	**1.2**	0.60	π/4	0.1	2.4395
2.0	0.5	π/6	4.0	2.0	**1.3**	0.60	π/4	0.1	2.4279
2.0	0.5	π/6	4.0	2.0	**1.4**	0.60	π/4	0.1	2.3582
2.0	0.5	π/6	4.0	2.0	1.0	**0.22**	π/4	0.1	2.7380
2.0	0.5	π/6	4.0	2.0	1.0	**0.78**	π/4	0.1	2.3690
2.0	0.5	π/6	4.0	2.0	1.0	**0.96**	π/4	0.1	2.3292

2.0	0.5	π/6	4.0	2.0	1.0	0.60	**π/12**	0.1	2.5663
2.0	0.5	π/6	4.0	2.0	1.0	0.60	**π/8**	0.1	2.4880
2.0	0.5	π/6	4.0	2.0	1.0	0.60	**π/3**	0.1	2.4271
2.0	0.5	π/6	4.0	2.0	1.0	0.60	π/4	**0.3**	2.3663
2.0	0.5	π/6	4.0	2.0	1.0	0.60	π/4	**0.4**	2.3113
2.0	0.5	π/6	4.0	2.0	1.0	0.60	π/4	**0.6**	2.2456

Table 2: The effects of various parameters on the Nusselt number

Pr	**ϕ**	**F**	**Nu**
0.7	0.1	**0.0**	0.8673
0.7	0.1	**1.0**	1.3776
0.7	0.1	**2.0**	1.7613
0.7	0.1	**3.0**	2.2887
0.72	0.1	1.0	1.4035
1.72	0.1	1.0	2.8416
2.72	0.1	1.0	3.5474
3.72	0.1	1.0	4.5931
0.7	**0.0**	1.0	1.3499
0.7	**0.1**	1.0	1.3776
0.7	**0.2**	1.0	1.4506
0.7	**0.3**	1.0	1.4578

Table 3: The effect of various parameters on the Sherwood number

γ	**Sc**	**Sh**
0.1	**0.22**	-0.2947
0.1	**0.60**	-0.6873
0.1	**0.78**	-0.8697
0.1	**0.96**	-1.0513
0.2	0.60	-0.7583
0.3	0.60	-0.8186
0.4	0.60	-0.8745

4. CONCLUSIONS

A theoretical analysis is performed to study the effects of thermal radiation, chemical reaction, Hall current and aligned magnetic on MHD flow of viscous, incompressible and electrically-conducting fluid on a moving inclined porous plate. Exact solutions of equations are obtained by perturbation technique. The conclusions of the study are as follows:

- Concentration decreases with increasing values of *Sc* and γ.
- Increase of ϕ, *Pr* and *F* lead to the decrease of temperature.
- Velocity increases with the increase of *Gr, Gc,* α, *F* and *K* and decreases with the increase of M, Sc, Pr, ξ, m and ϕ.
- Sherwood number decreases with increasing of *Sc* and γ.
- Nusselt number increases with increase of *Pr, F and* ϕ.
- As increasing of K, Gr, Gc causes the skin-friction coefficient increase and increasing of M, α, F, Sc, m and ξ, the skin-friction coefficient decreases.

REFERENCES

1. A. J. Chamkha, T. S. Reddy, M. C. Raju,and S. V. K. Varma, "unsteady MHD free convection flow past an exponentially accelerated vertical plate with mass transfer, chemical reaction and thermal radiation," International Journal of Microscale and Nanoscale Thermal and Fluid Transport Phenomena, vol. 5, pp. 57-75,2014.

2. D. A. S. Rees and I. Pop, "Vertical free convection in a porous medium with variable permeability effects," International Journal of heat mass transfer, 43, 2565-2571, 2010.

3. D. B. Ingham, I. Pop, and P. Cheng, "Combined free and forced convection in a porous medium between two vertical walls with viscous dissipation," Transp Porous Media, vol. 5, no. 4, pp. 381–398, 1990.

4. J. C. Umavathi, A. J. Chamkha, and A. Mateen, "Unsteady Oscillatory Flow and Heat Transfer in a Horizontal Composite Porous Medium Channel," Nonlinear Analysis: Modelling and Control, vol. 14, no. 3, pp. 397–415, 2009.

5. A. J. Chamkha, S. E. Ahmed, and A. S. Aloraier, "Melting and radiation effects on mixed convection from a vertical surface embedded in a non-Newtonian fluid saturated non-Darcy porous medium for aiding and opposing eternal flows," International Journal of the Physical Sciences, vol. 5, no. July, pp. 1212–1224, 2010.

6. M.A.Hossain,"Viscous and Joule heating effects on MHD-free convection flow with variable plate Temperature". International Journal of Heat and Mass Transfer, 35(12), 1992, 3485–3487.

7. M.A. Hossain, R.S. Gorla, “Joule heating effect on magnetohydrodynamic mixed convection boundary layer flow with variable electrical conductivity”, International Journal of Numerical Methods for Heat & Fluid Flow, Vol. 23(2), 275 – 288, 2013.
8. O.A. Bég, J. Zueco&H.S. Takhar, “Unsteady magnetohydrodynamic Hartmann–Couette flow and heat transfer in a Darcian channel with Hall current, ionslip, viscous and Joule heating effects: Network numerical solutions”, Communications in nonlinear science and numerical simulation, 14(4), 1082-1097, 2009.
9. C.H. Chen, “Combined heat and mass transfer in MHD free convection from a vertical surface with Ohmic heating and viscous dissipation”, International journal of engineering science, 42(7), 699-713, 2004.
10. N.A. Reddy, S.V.K. Varma, M. C. Raju, “Thermo diffusion and chemical effects with simultaneous thermal and mass diffusion in MHD mixed convection flow with Ohmic heating”, Journal of Naval Architecture and Marine Engineering, 6, 84-93, 2009.
11. P. Sibanda, O.D. Makinde, “On steady MHD flow and heat transfer past a rotating disk in a porous medium with Ohmic heating and viscous dissipation”, International Journal of Numerical Methods for Heat & Fluid Flow, 20 (3), 269 – 285, 2010.
12. A. Wang, C. Tu&X. Zhang, “Mixed convection of non-newtonian fluids from a vertical plate embedded in a porous medium”, ActaMechanicaSinica, 6 (3), 214-220, 1990.
13. K. A. Yih, “Viscous and Joule heating effects on non-Darcy MHD natural convection flow over a permeable sphere in porous media with internal heat generation”, International communications in heat and mass transfer, 27(4), 591-600, 2000.
14. R. Choudhury& S.K. Das, “Mixed Convective visco elastic MHD flow with Ohmic heating”, International Journal of computer applications, 68 (10), 7-13, 2013.
15. Raju M.C, C.Veeresh, S.V.K.Varma, Rushikumar B and Vijayakumar AG, “Heat And Mass Transfer In MHD Free Convection Flow on a Moving Inclined Porous Plate”, J Appl Computat Math ,4(5),1-7, 2015.